THROMBOSIS AND HEMOSTASIS

Kindlin-2 regulates hemostasis by controlling endothelial cell–surface expression of ADP/AMP catabolic enzymes via a clathrin-dependent mechanism

Elzbieta Pluskota,[1] Yi Ma,[1] Kamila M. Bledzka,[1] Katarzyna Bialkowska,[1] Dmitry A. Soloviev,[1] Dorota Szpak,[1] Eugene A. Podrez,[1] Paul L. Fox,[2] Stanley L. Hazen,[2] James J. Dowling,[3] Yan-Qing Ma,[4] and Edward F. Plow[1]

[1]Joseph J. Jacobs Center for Thrombosis and Vascular Biology, Department of Molecular Cardiology, and [2]Department of Molecular and Cellular Medicine, Cleveland Clinic, Cleveland, OH; [3]Departments of Pediatrics and Neurology, University of Michigan Medical Center, Ann Arbor, MI; and [4]Blood Research Institute, Blood Center of Wisconsin, Milwaukee, WI

Key Points

- Kindlin-2 regulates hemostasis in vivo by limiting CD39 and CD73 expression on the surface of endothelial cells.
- Kindlin-2 interacts directly with CHC and controls clathrin-dependent CD39 and CD73 endocytosis/recycling in endothelial cells.

Kindlin-2, a widely distributed cytoskeletal protein, has been implicated in integrin activation, and its absence is embryonically lethal in mice. In the present study, we tested whether hemostasis might be perturbed in *kindlin-2*$^{+/-}$ mice. Bleeding time and carotid artery occlusion time were significantly prolonged in *kindlin-2*$^{+/-}$ mice. Whereas plasma concentrations/activities of key coagulation/fibrinolytic proteins and platelet counts and aggregation were similar in wild-type and *kindlin-2*$^{+/-}$ mice, *kindlin-2*$^{+/-}$ endothelial cells (ECs) showed enhanced inhibition of platelet aggregation induced by adenosine 5′-diphosphate (ADP) or low concentrations of other agonists. Cell-surface expression of 2 enzymes involved in ADP/adenosine 5′-monophosphate (AMP) degradation, adenosine triphosphate (ATP) diphosphohydrolase (CD39) and ecto-5′-nucleotidase (CD73) were increased twofold to threefold on *kindlin-2*$^{+/-}$ ECs, leading to enhanced ATP/ADP catabolism and production of adenosine, an inhibitor of platelet aggregation. Trafficking of CD39 and CD73 at the EC surface was altered in *kindlin-2*$^{+/-}$ mice. Mechanistically, this was attributed to direct interaction of kindlin-2 with clathrin heavy chain, thereby controlling endocytosis and recycling of CD39 and CD73. The interaction of kindlin-2 with clathrin was independent of its integrin binding site but still dependent on a site within its F3 subdomain. Thus, kindlin-2 regulates trafficking of EC surface enzymes that control platelet responses and hemostasis. (*Blood*. 2013;122(14):2491-2499)

Introduction

Kindlins are cytoskeletal-associated proteins that have recently emerged as crucial regulators of integrin function.[1,2] The kindlins, along with talin, interact with the cytoplasmic tails of the β integrin subunits, and both are required to promote efficient integrin activation in vivo (reviewed in Plow et al[3] and Meves et al[4]). There are 3 kindlin family members in vertebrates, which are quite homologous, and sometimes even expressed within the same cell type.[3,5,6] However, the kindlins do not compensate for one another; deficiencies of each kindlin in mice and/or humans result in distinct phenotypes, indicative of their unique functions.[2-4,7-9]

Kindlin-2 is the most widely distributed of the 3 kindlin family members. Inactivation of the *kindlin-2* gene in mice is peri-implantation lethal by embryonic day 7.5 (E7.5).[10,11] Cells derived from kindlin-2–deficient mice[11] or cells in which kindlin-2 had been knocked down with small interfering RNA (siRNA) are defective in their ability to activate their integrins and consequently to adhere and migrate on integrin ligands.[6,12] Consistent with these observations, even partial reduction of kindlin-2 in *kindlin-2*$^{+/-}$ mice gives rise to impaired angiogenesis and defective activation of the β3 integrins in endothelial cells (ECs).[13]

Kindlin-2 is present in platelets[12] but is incapable of supporting the hemostatic functions of integrin αIIβ3 in kindlin-3–deficient platelets.[14] Thus, when we analyzed the *kindlin-2*$^{+/-}$ mice, we were surprised to detect prolonged bleeding and vascular occlusion times. In tracking the mechanism underlying defective hemostasis in these mice, we found that a reduced kindlin-2 level greatly enhances EC surface expression of 2 enzymes involved in adenine nucleotide catabolism: adenosine triphospate (ATP) diphosphohydrolase (CD39) and ecto-5′-nucleotidase (CD73). The elevated expression of these 2 enzymes on ECs suppresses platelet aggregation. Unexpectedly, this activity of kindlin-2 is independent of its integrin binding and is attributable to a previously unknown activity of kindlin-2: its capacity to regulate clathrin-dependent vesicle trafficking in ECs.

Methods

Kindlin-2$^{+/-}$ mice

The *kindlin-2*$^{+/-}$ mice were previously described, have normal fertility and litter sizes, and lack an overt phenotype.[10,15] Eight- to 12-week-old female

Submitted April 17, 2013; accepted July 15, 2013. Prepublished online as *Blood* First Edition paper, July 29, 2013; DOI 10.1182/blood-2013-04-497669.

The online version of this article contains a data supplement.

There is an Inside *Blood* commentary on this article in this issue.

The publication costs of this article were defrayed in part by page charge payment. Therefore, and solely to indicate this fact, this article is hereby marked "advertisement" in accordance with 18 USC section 1734.

and male mice were used, and *kindlin-2*$^{+/+}$ littermates served as controls. All procedures were performed under protocols approved by the Cleveland Clinic Institutional Animal Care and Use Committee.

Tail bleeding time and vascular occlusion analyses

Bleeding time and thrombosis assays were performed as previously described.[16] Tails were cut 3 mm from the tip and immersed in saline (37°C); the time it took for bleeding to stop was recorded. Calcein-labeled platelets were injected intravenously into syngeneic mice, and a 2 × 2 mm strip of filter paper saturated with 10% $FeCl_3$ was applied to the surface of the carotid artery for 2 minutes. The time from removal of the filter paper to complete flow cessation lasting for >20 seconds was measured.

Flow cytometry

Mouse platelets were incubated with phycoerythrin (PE)–rat anti-mouse CD41, fluorescein isothiocyanate (FITC)–rat anti-mouse P-selectin, PE-hamster anti-CD61 (BD Biosciences), hamster anti-mouse CD49b (Millipore), mouse anti-CD42b (Accurate Chemical). Mouse ECs were incubated with PE-conjugated rat anti-mouse CD39-PE, rat anti-mouse CD73-PE (eBioscience), FITC rat anti-mouse P-selectin, or isotype control antibodies (Abs), and analyzed on a FACSCalibur flow cytometer using CellQuest software (BD Biosciences).

Modulation of kindlin-2 expression in MAECs

Mouse aortic ECs (MAECs) were transfected with wild-type (WT) or previously described deletion mutants of kindlin-2[12] in a pEGFP-C2 construct (Clontech) using HCAEC nucleofector kits (Lonza). To reduce expression of kindlin-2, WT MAECs were transfected with siGenome SMARTpool mouse PLEKHC1 siRNAs and nontargeting siRNA#2 (Thermo Scientific Dharmacon) using Targefect human umbilical vein EC (HUVEC) reagents (Targeting Systems) according to the manufacturer's instructions. After 48 hours, the cells were subjected to fluorescence-activated cell sorter (FACS) analysis or CD39/CD73 activity assays.

Endocytosis assays

WT or *kindlin-2*$^{+/-}$ ECs were incubated in *N*-2-hydroxyethylpiperazine-*N*′-2-ethanesulfonic acid (HEPES) buffer (140 mM NaCl, 2.7 mM KCl, 0.1% BSA, 0.1% glucose, 3.8 mM HEPES, 1 mM $MgCl_2$, 1 mM $CaCl_2$, pH 7.5) with PE-conjugated anti-CD39 or anti-CD73 Abs (eBioscience) for 30 minutes at 4°C. Next, Abs were removed and cells were washed twice with ice-cold HEPES buffer. Cells were placed at 37°C, incubated for 0 to 2 hours, fixed in 4% paraformaldehyde and analyzed by FACS.

Immunoprecipitation

ECs lysates were precleared, incubated with anti-kindlin-2 monoclonal Ab (mAb) overnight at 4°C and incubated with Protein A/G-Sepharose (Santa Cruz Biotechnology) for 2 hours at 4°C. Sepharose beads were washed and analyzed on western blots with anti–clathrin heavy chain (CHC) and anti–kindlin-2 Abs. In some experiments, the kindlin-2 (583-604) peptide (ELIGIAYNRLIRMDASTGDAI) and its scrambled version were added to cell lysates, together with the anti-kindlin-2 Ab. To purify enhanced green fluorescent protein (EGFP)–tagged kindlin-2–associated proteins, Chinese hamster ovary (CHO) cell lysates were incubated with Chromotek GFP-Trap Sepharose (AlleleBiotech Innovative Technology) for 2 hours at 4°C. Sepharose-captured immunocomplexes were analyzed by western blot using anti-CHC and anti-GFP.

Surface plasmon resonance

The construct expressing clathrin N-terminal domain (1-363) as glutathione S-transferase (GST)–fusion protein was kindly provided by Dr Eileen Lafer (The University of Texas Health Science Center, San Antonio, TX).[17] GST-fused kindlin-2 and its mutants were purified by glutathione chromatography. Real-time protein-protein interactions were analyzed using a Biacore 3000 instrument. Clathrin N-terminal domain (CTD), upon removal of its GST tag, was immobilized on CM5 biosensor chips.[18] Experiments were performed at 22°C in 10mM HEPES buffer, pH 7.4, containing 150mM NaCl and 0.005% surfactant P20 (flow rate, 25 μL per minute). Surface plasmon resonance (SPR) sensograms were obtained by injecting various concentrations of GST-tagged kindlin-2 (1-680), kindlin-2 (1-105), kindlin-2 (95-680), kindlin-2 (281-541) over immobilized clathrin CTD and reference flow cells. Association/dissociation curves were determined after the subtraction of the reference surface values and buffer binding at 5 selected concentrations. Sensograms were analyzed using BIAevaluation software (version 4.01; GE Healthcare).

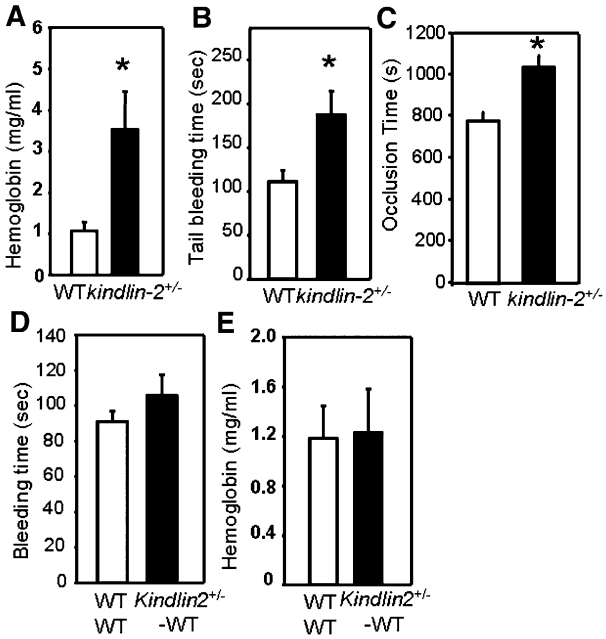

Figure 1. Prolonged bleeding and blood vessel occlusion time in *kindlin-2*$^{+/-}$ mice. (A) Total blood loss upon tail tip clip resection as measured by released hemoglobin using Drabkin reagent (n = 10). (B) Tail bleeding time as estimated after tail tip resection (n = 10 mice per group). (C) The time needed to form an occlusive thrombus in the carotid artery was determined in 10 control and 12 *kindlin-2*$^{+/-}$ mice after topical injury with $FeCl_3$. (D) Tail bleeding time and (E) total blood loss in WT recipients 6 weeks after bone marrow transplantation from WT or *kindlin-2*$^{+/-}$ donors.

Statistical analysis

Values are expressed as means ± SEM. Statistical significance was evaluated using a 2-tailed unpaired Student test or by nonparametric Mann-Whitney test for the intravital thrombosis experiments. Results were considered statistically significant with $P < .05$.

Results

Kindlin-2$^{+/-}$ mice have prolonged bleeding times and delayed thrombus formation

Although platelets contain low levels of kindlin-2,[12] it is not sufficient to fulfill the role of kindlin-3 in platelet hemostatic responses as kindlin-3 deficiency in mice and humans leads to significant bleeding phenotypes.[8,9,14] Thus, when we analyzed hemostasis in *kindlin-2*$^{+/-}$ mice with only a 50% reduction in kindlin-2 levels,[13] we were surprised to observe that total blood loss after tail tip resection, measured by hemoglobin content of collected blood, was enhanced by approximately fourfold in *kindlin-2*$^{+/-}$ mice compared with WT littermates ($P = .005$, n = 10 per group) (Figure 1A), and bleeding time was increased by ~70% in *kindlin-2*$^{+/-}$ animals ($P = .024$, n = 10 per group) (Figure 1B). Time to vessel occlusion, upon carotid artery injury with $FeCl_3$, was prolonged by ~30% in *kindlin-2*$^{+/-}$ mice compared with WT controls (n = 10 WT and 12 *kindlin-2*$^{+/-}$ mice, $P = .003$) (Figure 1C).

Plasma levels of several hemostatic factors, tissue plasminogen activator, plasminogen activator inhibitor-1, tissue factor pathway inhibitor, fibrinogen, and Von Willebrand factor, were measured and revealed no abnormalities in *kindlin-2*$^{+/-}$ mice. Peripheral blood platelet counts, platelet aggregation, and expression levels of key regulators of platelet activation also were similar in WT and *kindlin-2*$^{+/-}$ mice (supplemental Tables 1-3, available on the *Blood* website). Bone marrow transplantation experiments confirmed that the hemostatic defect in *kindlin-2*$^{+/-}$ mice was not a reflection of an abnormality in platelets or circulating coagulation factor interpretation; bleeding times and total blood loss were similar in WT recipients that received bone marrow either from WT or *kindlin-2*$^{+/-}$ donors ($P > .05$, n = 9 per group) indicating that hematopoietic cells, including platelets, do not contribute to bleeding in *kindlin-2*$^{+/-}$ mice (Figure 1D-E).

Kindlin-2$^{+/-}$ ECs exhibit enhanced anti-platelet activity

We compared the capacity of ECs isolated from WT and *kindlin-2*$^{+/-}$ mice to regulate platelet aggregation[19] by preincubating with increasing numbers of WT or *kindlin-2*$^{+/-}$ ECs in suspension with platelets isolated from WT and *kindlin-2*$^{+/-}$ mice followed by addition of adenosine 5′-diphosphate (ADP). In control experiments, we showed that (1) ECs gave a relatively stable baseline during a 10-minute incubation in the absence of platelets and (2) ECs from both WT and *kindlin-2*$^{+/-}$ mice did not interact spontaneously with platelets from either genotype during this incubation time. Both WT and *kindlin-2*$^{+/-}$ ECs inhibited ADP-induced platelet aggregation in a cell number–dependent manner (Figure 2A-B). However, the *kindlin-2*$^{+/-}$ ECs showed significantly enhanced platelet inhibitory activity compared with WT ECs. For example, in the absence of ECs, ~70% ± 7% platelets aggregated compared with 38% ± 4% platelet aggregation in the presence of WT ECs (1.4×10^6) while, in the presence of the same number of *kindlin-2*$^{+/-}$ ECs, only 8% ± 2% of platelets aggregated (Figure 2B left panel). There was no difference in the susceptibility of WT and *kindlin-2*$^{+/-}$ platelets to be inhibited by ECs of either WT or *kindlin-2*$^{+/-}$ origin (Figure 2B). *Kindlin-2*$^{+/-}$ ECs also showed increased inhibitory activity on platelet aggregation induced by low doses of other platelet agonists exemplified by collagen (1 μg/mL) or thrombin (0.05 U/mL) (Figure 2C) at agonist concentrations where released ADP influences platelet responses to these agonists.[20] However, at high concentrations of these agonists (collagen, 2 μg/mL; thrombin, 0.5 U/mL), the differential inhibitory effect of WT and *kindlin-2*$^{+/-}$ ECs on platelet aggregation was no longer observed (Figure 2C).

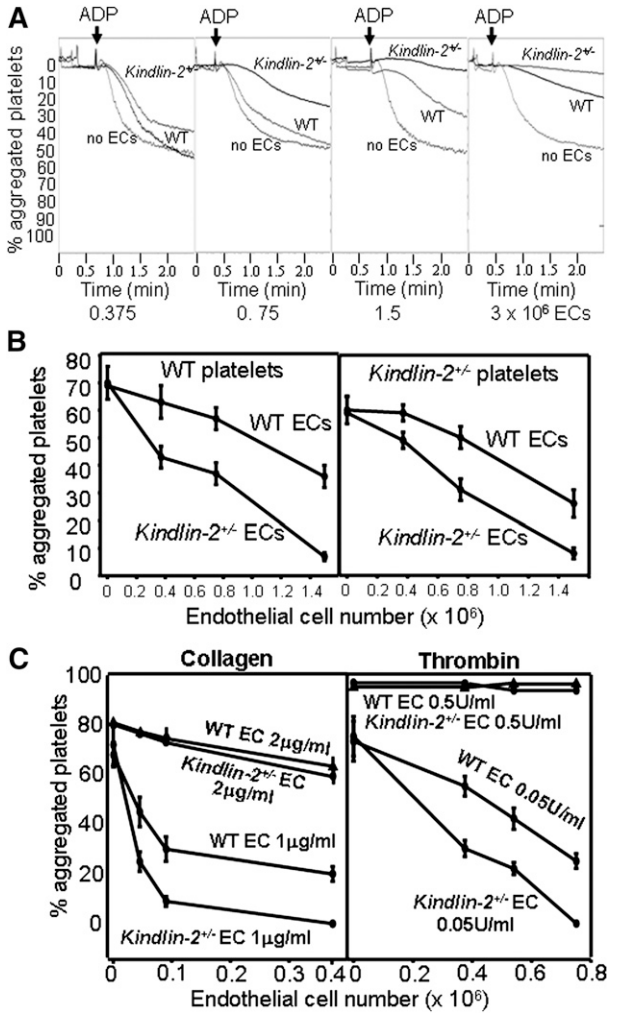

Figure 2. *Kindlin-2*$^{+/-}$ ECs show enhanced inhibition of platelet aggregation. (A) Representative tracings of platelet aggregation induced by ADP (10 μM) in the absence or presence of increasing numbers of WT or *kindlin-2*$^{+/-}$ ECs. Under the same conditions, thrombin (0.5 U/mL) induced 100% aggregation. (B) ADP-induced aggregation of WT and *kindlin-2*$^{+/-}$ platelets in the presence of WT or *kindlin-2*$^{+/-}$ ECs. The percentage of aggregated platelets was determined 4 minutes after addition of ADP. Data are mean ± SEM (n = 9) and are representative of 3 independent experiments. (C) Effect of WT and *kindlin-2*$^{+/-}$ ECs on aggregation of WT platelets induced by collagen (1 and 2 μg/mL) or thrombin (0.05 and 0.5 U/mL). Data show the percentage of aggregated platelets 5 minutes after agonist addition and are means ± SEM (n = 3) from 2 independent experiments.

Enhanced expression of CD39 and CD73 contributes to augmented anti-platelet activity of *kindlin-2*$^{+/-}$ endothelium

ECs execute their anti-platelet properties via 3 distinct mechanisms: endothelial nitric oxide synthase (eNOS)–dependent NO production,[19] biosynthesis of prostacyclins,[21] or regulation of ADP and adenosine levels via cell-surface NTPDase (CD39)[22] and 5′-ectonucleotidase (CD73).[22,23] We compared all 3 anti-platelet pathways in WT and *kindlin-2*$^{+/-}$ ECs. eNOS expression and phosphorylation and prostacyclin release in ECs from both genotypes were similar (data not shown), whereas FACS revealed significantly increased (twofold to threefold) CD39 and CD73 expression on the surface of *kindlin-2*$^{+/-}$ ECs compared with WT ECs (Figure 3A-B). However, cell-surface expression of intercellular adhesion molecule-1 (ICAM-1) and P-selectin was the same in WT and *kindlin-2*$^{+/-}$ ECs.

We next measured the activities of these adenine nucleotide catabolic enzymes on WT and *kindlin-2*$^{+/-}$ ECs. The ADP-ase activity of CD39 was measured as release of inorganic orthophosphate (P_i) from ADP into EC supernatants over time. To help ensure that P_i was released from ADP, the experiments were performed in the presence of CD73 inhibitor adenosine 5′-(α,β-methylene)diphosphate to block P_i cleavage from adenosine 5′-monophosphate (AMP) and levamisole, the alkaline phosphatase inhibitor. In control samples, when ECs were incubated in the absence of ADP, background levels of P_i were extremely low. At every time point, CD39 activity was significantly augmented (twofold to threefold) on the surface of *kindlin-2*$^{+/-}$ ECs compared with WT ECs (Figure 3C). To further confirm that *kindlin-2*$^{+/-}$ ECs metabolized ADP more efficiently than WT ECs, ADP was added to ECs, and at various times the conditioned media was used to stimulate platelet aggregation, that is, the residual ADP (not hydrolyzed by CD39) served as the platelet agonist. The capacity of EC supernatants to induce platelet aggregation decreased proportionally with cell number and ADP:EC incubation time (Figure 3D). However, at every time point, the conditioned medium from *kindlin-2*$^{+/-}$ ECs was twofold to eightfold less

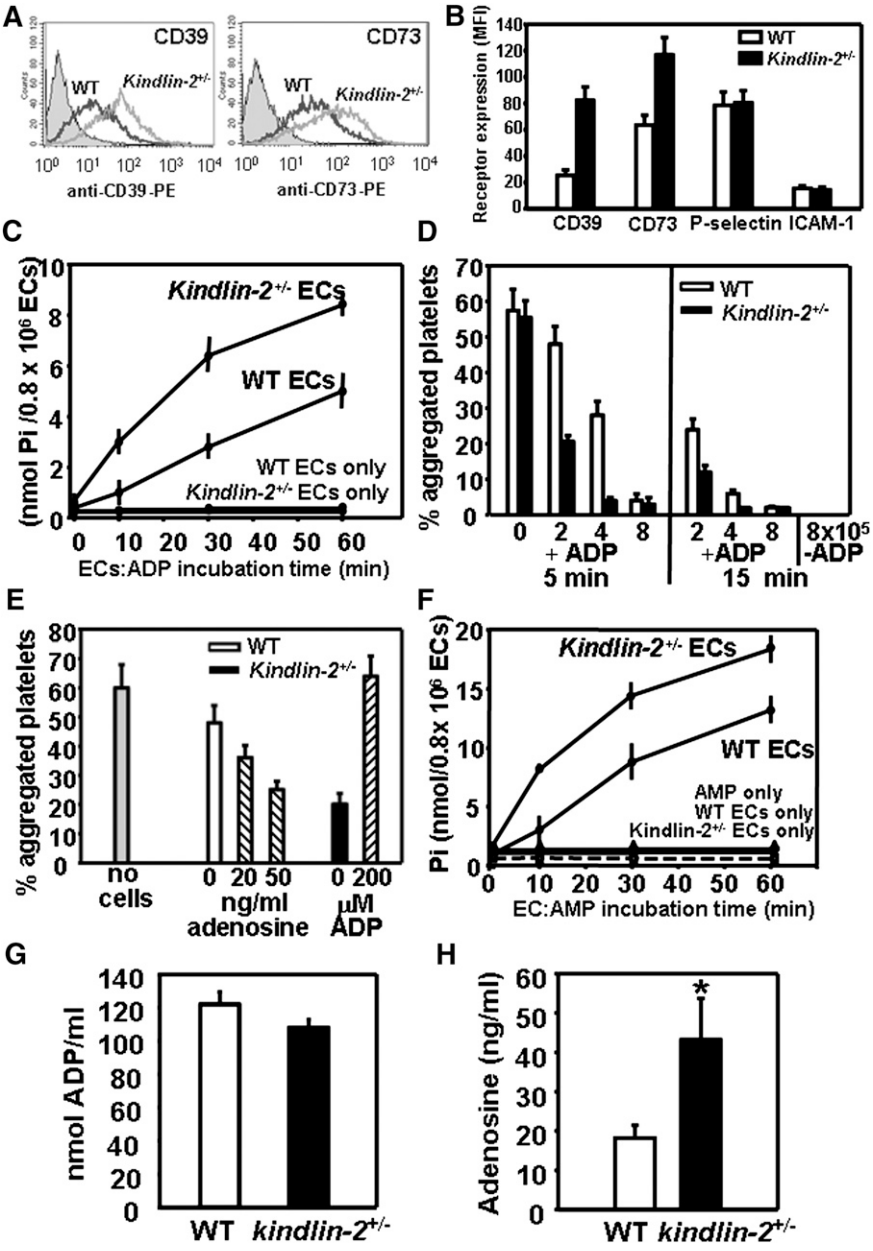

Figure 3. CD39 and CD73 expression levels and enzymatic activities are significantly increased on the surface of *kindlin-2*$^{+/-}$ ECs. (A) Representative FACS analysis of WT and *kindlin-2*$^{+/-}$ ECs stained with PE-conjugated Abs to CD39 and CD73. Gray-filled histograms represent isotype controls. (B) FACS analyses of WT (□) and *kindlin-2*$^{+/-}$ (■) ECs stained with Abs to CD39, CD73, P-selectin, and ICAM-1. The data are mean ± SEM of triplicate samples and are representative of 4 independent experiments. (C) CD39 activity on the surface of WT and *kindlin-2*$^{+/-}$ ECs. ECs (8×10^5) were incubated in the absence or presence of substrate ADP (100 μM) for 0 to 60 minutes at 37°C in the presence of adenosine 5′-(α,β-methylene)diphosphate, the CD73 inhibitor. Concentration of inorganic P_i released from ADP in EC supernatants was measured using malachite green assay. (D) Platelet aggregation induced by remaining (not hydrolyzed by CD39) ADP present in the supernatants of WT (□) or *kindlin-2*$^{+/-}$ (■) ECs (0-8×10^5) treated with ADP (100 μM) for 5 or 15 minutes; in controls, no ADP was added. (E) Platelet aggregation induced by ADP present in the supernatants of WT (□) or *kindlin-2*$^{+/-}$ (■) ECs (2×10^5) treated with ADP (100 μM) for 5 minutes. Adenosine (0-50 ng/mL) was added to WT EC-conditioned medium, while ADP (200 μM) was added to kindlin-2$^{+/-}$ EC-conditioned medium. (F) CD73 activity on the surface of WT or *kindlin-2*$^{+/-}$ ECs. ECs (8×10^5) were incubated in the absence or presence of substrate AMP (100 μM) for 0 to 60 minutes in the presence of the alkaline phosphatase inhibitor levamisole. P_i formed from AMP in EC supernatants was measured using a malachite green assay kit. Data are mean ± SEM of triplicate samples from 3 independent experiments. ADP (G) and adenosine (H) concentrations in plasma of WT and *kindlin-2*$^{+/-}$ mice were measured as described in "Methods." Results are expressed as mean ± SEM from 7 to 10 mice per group. MFI, mean fluorescence intensity.

effective in triggering platelet aggregation than that from WT ECs (Figure 3D). In control samples, EC-conditioned medium without ADP added did not trigger platelet aggregation (Figure 3D).When excess ADP (200 μM) was added to *kindlin-2*$^{+/-}$ EC-conditioned medium, the effect of increased ADP hydrolysis was overcome, and platelet aggregation was restored to levels observed in samples without ECs present (Figure 3E). Adenosine, the product of CD73-mediated hydrolysis of AMP, reduced platelet aggregation induced by WT EC-conditioned medium by 50%, confirming the inhibitory effect of adenosine on platelet aggregation (Figure 3E). Next, CD73 activity was measured using AMP as the substrate; the CD73 activity was also approximately twofold higher on *kindlin-2*$^{+/-}$ ECs than on WT ECs. In control samples, when ECs were incubated in the absence of adenine nucleotides, no P_i was detected in the supernatants indicating that the cells did not release P_i (Figure 3F). Consistent with the increase in CD73 levels on *kindlin-2*$^{+/-}$ ECs, plasma adenosine was significantly increased in *kindlin-2*$^{+/-}$ mice (18.12 ± 3.29 in WT, 43.13 ± 10.54 ng/mL in *kindlin-2*$^{+/-}$ mice, n = 10, $P = .036$) (Figure 3G-H). However, ADP levels were similar in plasma of WT and *kindlin-2*$^{+/-}$ mice.

Kindlin-2 regulates CD39 and CD73 expression on the endothelial surface

We sought to obtain direct evidence that kindlin-2 regulates expression of CD39 and CD73 in ECs. Band densities from western blots of EC lysates revealed that kindlin-2 expression was decreased by ~50% to 60% in WT ECs treated with kindlin-2 targeting siRNA compared with untreated or treated with control siRNA WT ECs. Upon reduction, kindlin-2 expression in WT cells was similar to that of *kindlin-2*$^{+/-}$ ECs (Figure 4A). The decrease of kindlin-2 expression in WT ECs resulted in a substantial increase (twofold to threefold) in cell surface expression and enzymatic activities of both enzymes in these cells. Control siRNA failed to affect CD39 and

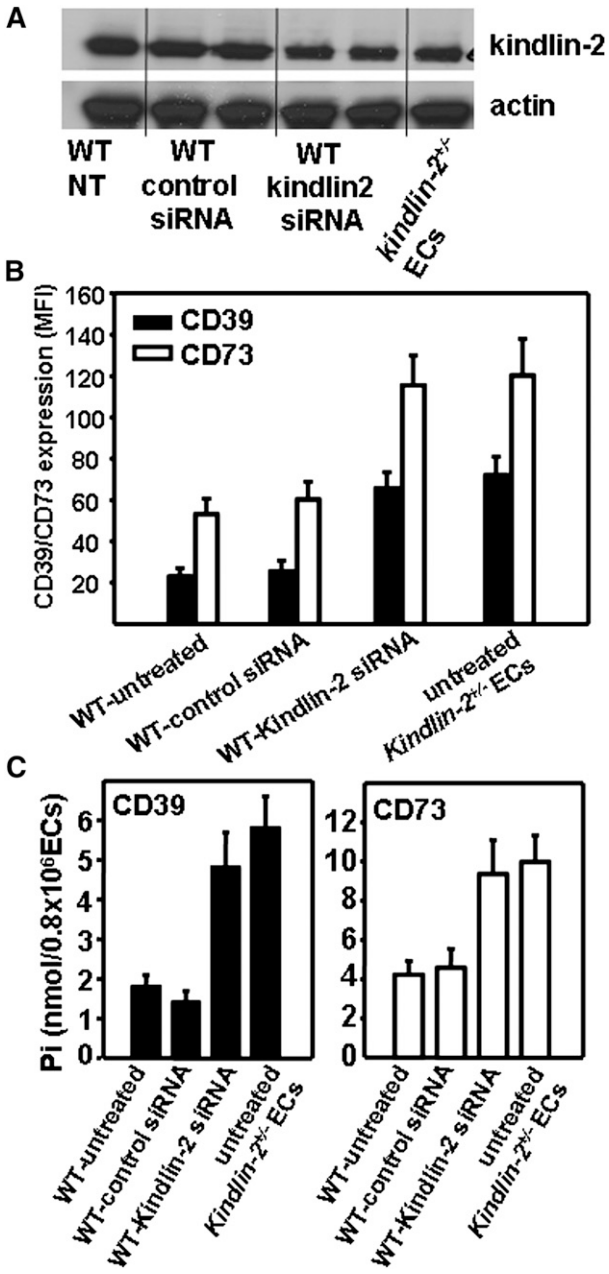

Figure 4. Reduction of kindlin-2 expression in WT ECs results in enhanced CD39 and CD73 expression and activities. WT and *kindlin-2*$^{+/-}$ ECs were either untreated or treated with control or kindlin-2 siRNA. Untreated *kindlin-2*$^{+/-}$ ECs served as control. (A) Western blot analysis of EC lysates using anti–kindlin-2 mAbs or Abs to actin as a loading control. (B) FACS analysis with anti-CD39 and anti-CD73 Abs reveal reduced CD39 and CD73 expression on kindlin-2 siRNA-treated WT ECs. The data are mean ± SEM of triplicate samples and are representative of 3 independent experiments. (C) CD39 (left panel) and CD73 (right panel) activities were analyzed on the EC surface as described in Figure 3C. The data are mean ± SEM of quadruple samples of 3 independent experiments. NT, nontreated.

CD73 expression and activity (Figure 4B-C). When we attempted to further inhibit kindlin-2 expression in *kindlin-2*$^{+/-}$ ECs and analyze CD39 and CD73 activity, the cells detached and failed to exclude trypan blue, likely a consequence of defective integrin function.

Altered clathrin-dependent trafficking enhances expression of CD39 and CD73 on *kindlin-2*$^{+/-}$ ECs

Western blot and reverse transcription–polymerase chain reaction assays revealed that both messenger RNA and total protein levels of CD39 and CD73 are similar in WT and *kindlin-2*$^{+/-}$ ECs (Figure 5A, supplemental Table 4). These results suggest that higher CD39/CD73 expression on the surface of *kindlin-2*$^{+/-}$ ECs may result from altered trafficking or recycling of these 2 enzymes. We compared the kinetics of CD39 and CD73 internalization in WT and *kindlin-2*$^{+/-}$ ECs. Not only did twofold to fourfold more CD39 and CD73 internalize into WT ECs as compared with *kindlin-2*$^{+/-}$ ECs within the first 15 minutes, but also their recycling to the surface was much slower in WT ECs (Figure 5B-C).

To identify the protein transport pathway involved in CD39 and CD73 trafficking, we stained WT ECs for CD39 or CD73 and for established markers of protein vesicular transport: clathrin, caveolin,

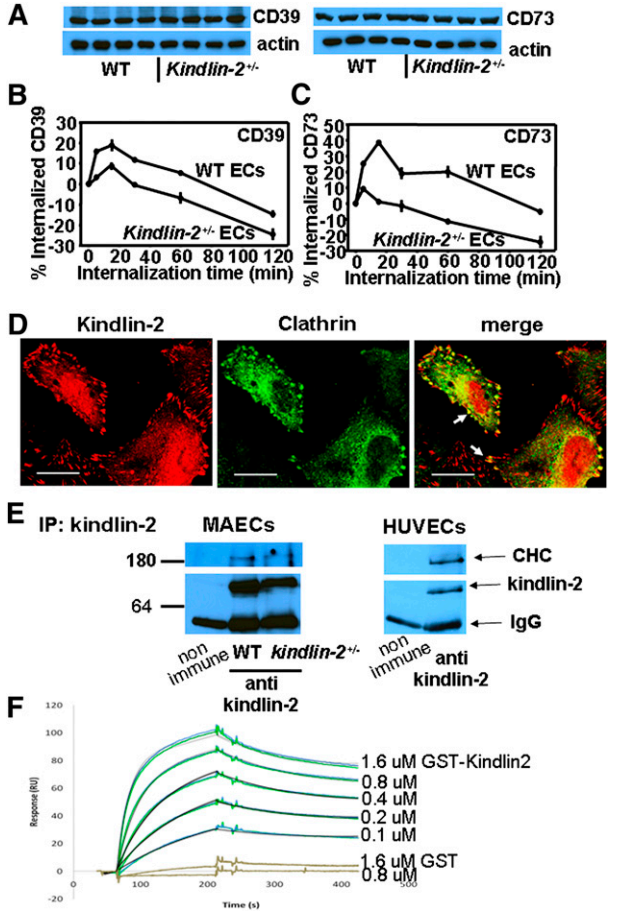

Figure 5. Defective clathrin-dependent trafficking of CD39 and CD73 in *kindlin-2*$^{+/-}$ ECs. (A) Western blot analysis of WT and *kindlin-2*$^{+/-}$ EC lysates probed with Abs to CD39 and CD73 reveal similar total content of these enzymes in both mouse strains (top panel). The blots were reprobed with Ab to actin to confirm equal protein loading (bottom panel). (B-C) Comparison of kinetics of CD39 (B) and CD73 (C) internalization in WT and *kindlin-2*$^{+/-}$ ECs. The measurements were performed as described in "Methods." The data are mean ± SEM of triplicate samples and are representative of 3 independent experiments. (D) Kindlin-2 and clathrin colocalization in WT ECs. The cells were stained with mAbs to kindlin-2 followed by Alexa 568–coupled goat anti-mouse IgG (red fluorescence) and rabbit anti-clathrin Ab and Alexa 488–conjugated goat anti-rabbit IgG (green fluorescence). Immuno-Fluore mounting medium (MPI Biomedicals) was used to mound the slides, and the images were taken with a 63 × 1.4 oil objective using a Leica TCS-NT laser scanning confocal microscope and Leica confocal software (version 2.5, build 1227). Images are representative of 3 independent experiments (bar size, 20 μm). Arrows point to focal adhesions. (E) Clathrin coimmunoprecipitates with kindlin-2 from EC lysates. Kindlin-2 was immunoprecipitated from lysates of MAECs (left panel) and HUVECs (right panel). Immunoprecipitates were analyzed on western blots with Abs to CHC and kindlin-2 as indicated. Images are representative of 3 independent experiments. (F) The CTD (1-363) was immobilized on the CM5 sensor chip surfaces (500 RU). Sensograms obtained for a concentration series of GST-kindlin-2 or GST protein (each concentration measured twice and shown as colored lines) were fit to a 1:1 interaction model with a drifting baseline (shown as black lines). Ig, immunoglobulin; IP, immunoprecipitation; RU, response units.

and the endosomal markers Rab4, Rab5, and 11. Of these, clathrin (red fluorescence) showed the strongest colocalization with both enzymes (green fluorescence) in ECs (supplemental Figure 1A-B). When chlorpromazine and methylamine, inhibitors of clathrin-mediated endocytosis,[24] were added, CD39 and CD73 expression on the surface of WT and kindlin-$2^{+/-}$ ECs was augmented by twofold to 2.5-fold as compared with untreated cells. In contrast, brefeldin A, which changes Golgi structure and inhibits recruitment of clathrin adaptors into Golgi membranes,[25] had no effect on CD39 or CD73 expression in ECs (supplemental Figure 1C-D).

Kindlin-2 colocalizes and interacts directly with the CTD

When WT ECs were stained for kindlin-2 (red fluorescence) and clathrin (green fluorescence), the 2 proteins colocalized not only at focal adhesions (shown by arrows) but also in proximity to clathrin-coated vesicles (Figure 5D). Furthermore, CHC coimmunoprecipitated with kindlin-2 from the lysates of murine and human ECs, indicating that clathrin and kindlin-2 coassociate (Figure 5E). To determine whether kindlin-2 interacts directly with the N-terminal domain of CHC (CTD), the major binding site for most of its adaptor and accessory proteins during clathrin-coated pits formation,[26,27] we performed SPR. Kindlin-2 interacted with CTD (GST tag removed) immobilized on the biosensor chip in a concentration-dependent manner (Figure 5F). The interaction between GST alone and CTD was negligible. From the progress curves of the kindlin-2:CTD interaction, we estimated a $K_d = 1.3 \times 10^{-7}$ M. This value was derived by fitting the kinetic data to a 1:1 global Langmuir model, and the stoichiometry observed at ligand saturation was 1:1, suggesting that the single binding site model was appropriate.

To determine which region(s) of kindlin-2 interacts with CTD, kindlin-2 fragments N terminus kindlin-2 (1-105), kindlin-2 (95-680), and kindlin-2 (281-541) were expressed as GST-tagged proteins, purified, and used in SPR studies. As shown in Figure 6A, kindlin-2 (95-680) bound CTD as efficiently as the full-length kindlin-2 (1-680) while the kindlin-2 (281-541) fragment did not bind, locating a major CTD binding site to the 542-680 region containing the F3 subdomain. The kindlin-2 (1-105) fragment also bound CTD but to a much lesser extent than F3, suggesting that the N-terminal aspect of kindlin-2 may assist in CTD recognition (Figure 6A). Sequence analysis of the kindlin-2 (542-680) fragment predicted a putative clathrin binding sequence (593)LIRMD(597), similar to a clathrin box motif, LΦXΦD/E, which is composed of polar amino acid residues (ΦXΦ) flanked by hydrophobic (L) and acidic amino acid residues (D/E).[26,27] To determine whether this putative clathrin binding site in kindlin-2 is functional, we expressed kindlin-2 deletion mutants lacking individual subdomains (ΔF0,ΔF1,ΔF2, and ΔF3), a clathrin box deletion mutant lacking residues 593-597 (Δ593-597) within the F3 subdomain, and a $Q^{614}W^{615}$/AA mutant that cannot bind integrin β subunits.[12] These mutant forms of kindlin-2 were immunoprecipitated with anti-GFP from CHO cell lysates and analyzed by western blots with Abs to CHC and GFP. WT kindlin-2 and most of its mutants coimmunoprecipitated with CHC, with the exception of mutants lacking either the F3 subdomain(Δ567-652) or the clathrin box LIRMD motif (Δ593-597) (Figure 6B).

These studies were extended using a synthetic peptide corresponding to residues 584-604 of kindlin-2 containing the putative clathrin box motif. When added to EC lysates, the kindlin-2 peptide reduced the association of CHC with kindlin-2 in a dose-dependent fashion (Figure 6C). By densitometry, 50μM peptide reduced CHD pull-down with anti–kindlin-2 by >96%, whereas a scrambled control peptide reduced coimmunoprecipitation by <10% (Figure 6C).

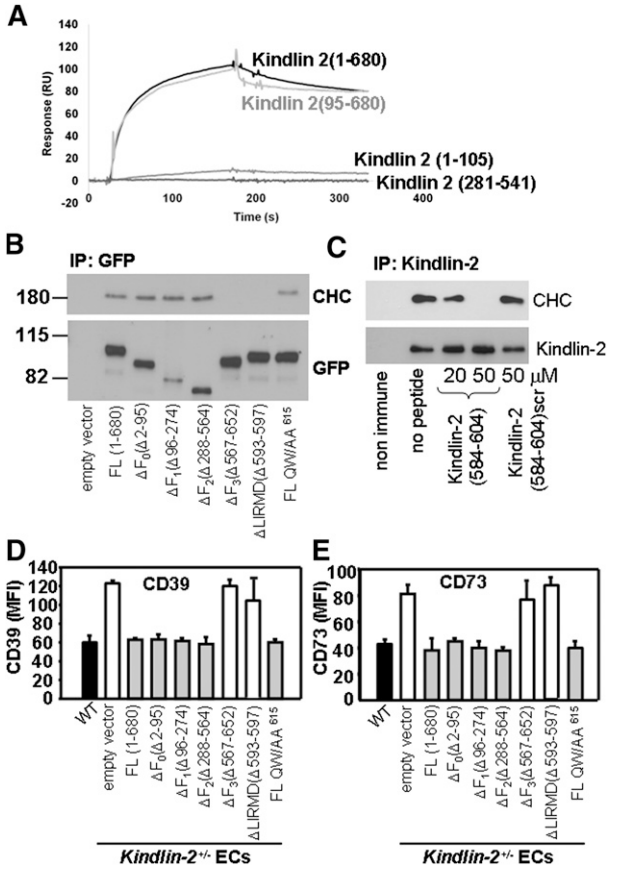

Figure 6. Clathrin interacts with clathrin box sequence within the F3 domain of kindlin-2. (A) Representative binding of 1 concentration (1.6 μM) of the following full-length kindlin-2 (1-680) and kindlin-2 fragments: (1-105), (95-680), and (281-541) to clathrin TD domain (1-363). The clathrin TD domain was immobilized on the CM5 sensor chip surfaces (~500 RU). (B) EGFP-tagged WT and mutants of kindlin-2 were immunoprecipitated from lysates of CHO cells transfected with the respective kindlin-2 constructs (as shown) using GFP-Trap Sepharose. The binding of clathrin to kindlin-2 mutants was analyzed on western blots with Abs to CHC. Kindlin-2 expression levels are revealed with anti-GFP Ab. The results are representative of 3 independent experiments. (C) Kindlin-2 was immunoprecipitated from WT ECs in the absence or presence of a peptide corresponding to residues 584-604 of kindlin-2 or its scrambled version followed by western blot analysis with anti-CHC and anti–kindlin-2 Abs. The images are representative of 2 experiments. (D-E) Overexpression of ΔF3 or Δ(LIRMD) deletion mutants of kindlin-2 does not reduce surface expression of CD39 and CD73 in *kindlin-2*$^{+/-}$ ECs. The cells were transfected with the EGFP constructs of WT, QW/AA^{615}, deletion mutants of kindlin-2, or empty EGFP vector as indicated. Cell-surface expression of CD39 (D) and CD73 (E) were measured using PE-conjugated anti-CD39 and anti-CD73 Abs by FACS analysis of the $EGFP^+$ cell population. The data represent mean ± SEM of triplicate samples and are representative of 3 independent experiments.

Further support for involvement of the kindlin-2 in clathrin-mediated regulation of CD39 and CD73 surface expression was derived from experiments in which EGFP-tagged kindlin-2 mutants were expressed in *kindlin-2*$^{+/-}$ ECs. When the *kindlin-2*$^{+/-}$ ECs were transfected with WT kindlin-2, FACS analysis of EGFP-positive cells revealed that cell-surface expression of CD39 and CD73 was reduced to levels detected on WT ECs (Figure 6D-E). Several other mutants of kindlin-2, ΔF0, ΔF1, and ΔF2 also caused a similar reduction in CD39 and CD73 expression. In contrast, the kindlin-2 mutants lacking the F3 subdomain (ΔF3) or the residues 593-597 (Δ593-597) failed to rescue the phenotype and did not decrease CD39/CD73 expression in *kindlin-2*$^{+/-}$ ECs. Furthermore, even though the $Q^{614}W^{615}$/AA kindlin-2 mutant does not bind to integrin,[12,13] it was as effective as WT kindlin-2 in decreasing CD39 and CD73 levels (Figure 6D-E). The integrin independence of CD39/CD73 expression

was further corroborated by FACS. CD39 and CD73 levels were similar on ECs isolated from WT mice and mice deficient in β_3 integrin (supplemental Figure 2).

Discussion

Our studies show that kindlin-2 is crucial in hemostasis. This conclusion is supported by in vivo experiments performed in *kindlin-2*$^{+/-}$ mice where we observed enhanced bleeding upon tail resection and prolonged occlusion time upon $FeCl_3$ injury. Perturbations of hemostasis are most frequently assigned to abnormalities in the concentration or function of key coagulation and fibrinolytic proteins or to suppression in platelet number and responses, but these were normal in *kindlin-2*$^{+/-}$ mice. Instead, it was ECs that showed a dysfunction. The capacity of ECs to inhibit platelet activation and intravascular thrombosis is well established (reviewed in Robson[19]). *Kindlin-2*$^{+/-}$ ECs displayed an enhanced capacity to inhibit platelet aggregation induced by ADP and low doses of other agonists. This dysfunction arose from enhanced expression of CD39 and CD73 leading to accelerated removal of the platelet agonist, ADP, and increased production of an aggregation inhibitor, adenosine. Measurement of P_i using malachite green supported this conclusion. Even though this assay was performed under conditions that favored ADP and AMP as the source of the P_i, we cannot fully exclude that the P_i might also be generated by other substrates.

The phenotype of *kindlin-2*$^{+/-}$ mice with increased CD39 activity is consistent with that of transgenic mice overexpressing human CD39 which also display prolonged bleeding times and reduced thrombus formation.[28-30] Paradoxically, *CD39*$^{-/-}$ mice have a bleeding phenotype similar to that of *kindlin-2*$^{+/-}$ mice, but this has been attributed to defective platelet aggregation caused by desensitization of purinoreceptors.[31] We found no evidence of a defect in *kindlin-2*$^{+/-}$ mouse platelets. We did not detect reduced levels of plasma ADP in *kindlin-2*$^{+/-}$ mice, and reduced ADP levels were also not noted in CD39-deficient mice,[31] suggesting that it is probably the ADP within the immediate milieu of the injured endothelium that regulates platelet responses. The phenotype of *CD73*$^{-/-}$ mice is attributable to low adenosine levels and, as expected, is the opposite of that observed in *kindlin-2*$^{+/-}$ mice.[32] Consistent with enhanced CD73 expression, adenosine levels were significantly increased in plasma of *kindlin-2*$^{+/-}$ mice. As enhanced adenosine was also detected in plasma of transgenic mice overexpressing human CD39, ADP may be rapidly converted to adenosine and it is probably the high levels of adenosine that are primarily responsible for the bleeding and anti-thrombotic phenotype of *kindlin-2*$^{+/-}$ mice.[29]

Kindlin-2$^{+/-}$ ECs showed an enhanced capacity to inhibit platelet aggregation induced by ADP and low doses of thrombin and collagen, but not by high concentrations of these 2 agonists. It is known that low-dose thrombin and collagen induce ADP secretion from platelets, which enhances fibrinogen binding and platelet aggregation[20]; at high agonist concentrations, platelet aggregation becomes ADP independent.[33] The ability of higher agonist concentrations to overcome the inhibitory effect of ECs is consistent with the greater effect of *kindlin-2*$^{+/-}$ ECs with their enhanced ectonucleotidase activities at the lower doses of agonists. However, we cannot exclude that factors other than ADP released from platelets may also influence the aggregation response.

Although bleeding in *kindlin-2*$^{+/-}$ mice is relatively modest, it is similar to that observed in P-selectin–, FXI-, and FXII-deficient mice.[34,35] Like the *kindlin-2*$^{+/-}$ mice, these mice do not bleed spontaneously but have prolonged bleeding times and reduced thrombosis when challenged. It should also be emphasized that the hemostatic defect in *kindlin-2*$^{+/-}$ mice is caused by only a 50% reduction in kindlin-2 levels.[13] Many mouse strains with severe bleeding associated with full gene deletion (eg, TF) exhibit no bleeding in the hemizygous state.[36]

In seeking a mechanism for the enhanced expression of CD39/CD73 on *kindlin-2*$^{+/-}$ ECs, we noted that the internalization and recycling of these enzymes was impaired, thereby increasing their cell-surface expression. Very limited information is available on the protein transport pathways regulating CD39 and CD73 trafficking. Our implication of clathrin in their surface expression was unexpected; it had been suggested that CD39 localized to caveolae[37] and, as a glycosylphosphatidylinositol-anchored protein, CD73 trafficking would be clathrin independent. Nevertheless, CD39 does contain a common clathrin-dependent internalization signal within its cytoplasmic domain, and our colocalization of CD73 with clathrin-coated vesicles is consistent with the clathrin-dependent transport of several other proteins lacking cytoplasmic domains.[38-40] Furthermore, well-accepted inhibitors of clathrin-mediated transport, chlorpromazine and methylamine, enhanced expression of CD39 and CD73 at the EC surface. We do not exclude that the transport of these enzymes to the cell surface may also involve clathrin-independent pathways, including pathways not regulated by kindlin-2. The clathrin inhibitors enhanced surface expression of CD39 and CD73 on both WT and *kindlin-2*$^{+/-}$ ECs. This may reflect the suboptimal concentrations of the inhibitors or the contributions of these other pathways. The basis for the differential expression of CD39 and CD73 on both WT and *kindlin-2*$^{+/-}$ ECs treated with the clathrin inhibitors remains to be resolved in future experiments, as does the question as to whether kindlin-2 regulation of clathrin-dependent internalization is limited only to CD39 and CD73. As an initial look at this latter issue, we examined the expression levels of the major ADP receptor on ECs, the G-protein–coupled P2Y1 receptor. By FACS, its expression was also enhanced by twofold to threefold on the surface of *kindlin-2*$^{+/-}$ EC as compared with WT cells (supplemental Figure 3). Thus, the role of kindlin-2 in trafficking of membrane proteins may be quite broad.

Kindlin-2 not only colocalized and immunoprecipitated with clathrin in ECs but also interacted directly with the N-terminal domain of CHC, which provides binding sites for most of its adaptor and accessory proteins. The clathrin binding site in kindlin-2 mapped to the F3 subdomain. During formation of clathrin-coated pits and vesicles, clathrin cannot interact directly with plasma membrane or cargo proteins and uses a variety of adaptor and accessory proteins to be recruited to the plasma membrane and bind cargo. The majority of these proteins bind to the N-terminal domain of clathrin and recruit clathrin to the membrane phospholipid bilayer through their PIP2 ($PtdIns(4,5)P_2$) binding domains.[26,41] Kindlin-2, which engages its F3 subdomain to regulate clathrin-dependent CD39/CD73 transport and has the capacity to interact with the membrane phosphoinositides via its pleckstrin homology domain and additional lipid binding sites,[42,43] conforms in properties to most clathrin adaptor/accessory proteins. How kindlin-2 participates in clathrin vesicle formation will require future investigations.

The most extensively characterized function of the kindlins is their role in integrin activation.[3,5,11] Both *kindlin-2*$^{+/-}$ and β3 integrin-KO mice show enhanced bleeding and reduced thrombosis. However, the mechanisms accounting for these overlapping phenotypes are different. Impaired platelet aggregation leads to bleeding in the β3-KO mice,[44] while in *kindlin-2*$^{+/-}$ mice platelets are normal and EC dysfunction confers anti-platelet activity. Although activation of the β3 integrins is reduced in *kindlin-2*$^{+/-}$ ECs,[13] this defect is not

responsible for enhanced CD39/CD73 expression because (1) ECs isolated from β3-KO and WT mice have similar CD39/CD73 surface expression/activity and (2) the kindlin-2 QW^{615}/AA mutant did not suppress CD39/CD73 expression in *kindlin-2*$^{+/-}$ ECs. The bleeding phenotype in *kindlin-2*$^{+/-}$ mice appears to be the first clear demonstration of an integrin-independent role of kindlin-2 in vivo.

Enhanced CD39 activity, either by overexpression of human CD39 or administration of soluble CD39, conferred resistance to systemic thromboembolism, inhibited platelet aggregation, and reduced cerebral infarct volumes in mice.[28-30,45,46] Our studies of *kindlin-2*$^{+/-}$ mice suggest that even partial inhibition of kindlin-2 may blunt platelet hyperreactivity and therefore represents a potential therapeutic target.

Acknowledgments

The authors thank Dr Judy Drazba and the Cleveland Clinic Imaging Core for assistance. The authors also kindly thank Dr Eileen M. Lafer for the gift of the NTD-Clathrin-GST construct and valuable comments on the manuscript, and Dr Jun Qin for the kindlin-2 (1-105) construct.

This work was supported by National Institutes of Health grants from the Heart, Lung, and Blood Institute (P01 HL 073311 and R01 HL096062 to E.F.P.) and from the National Institute of Allergy and Infectious Diseases (NIAID) (AIO 80596 to D.A.S.). HUVECs were made available by National Center for Advancing Translational Sciences (NCATS) grant UL1TR000439 to the Clinical and Translational Science Collaborative of Cleveland.

Authorship

Contribution: E.P. designed and performed experiments, analyzed and interpreted data, and wrote the paper; J.J.D. provided the kindlin-2$^{+/-}$ and WT mice; Y.M., K.M.B., K.B., D.A.S., and D.S. performed experiments and analyzed data; E.A.P. interpreted data, and assisted as an expert in thrombosis; P.L.F. and S.L.H. analyzed data and edited the manuscript; Y.-Q.M. provided essential constructs; E.F.P. designed, coordinated, and supervised research, and wrote the paper; and all authors critically reviewed the manuscript.

Conflict-of-interest disclosure: The authors declare no competing financial interests.

Correspondence: Edward F. Plow, Department of Molecular Cardiology, Lerner Research Institute, Cleveland Clinic, 9500 Euclid Ave, NB50, Cleveland, OH 44195; e-mail: plowe@ccf.org.

References

1. Moser M, Legate KR, Zent R, Fässler R. The tail of integrins, talin, and kindlins. *Science.* 2009; 324(5929):895-899.
2. Larjava H, Plow EF, Wu C. Kindlins: essential regulators of integrin signalling and cell-matrix adhesion. *EMBO Rep.* 2008;9(12): 1203-1208.
3. Plow EF, Qin J, Byzova T. Kindling the flame of integrin activation and function with kindlins. *Curr Opin Hematol.* 2009;16(5):323-328.
4. Meves A, Stremmel C, Gottschalk K, Fässler R. The Kindlin protein family: new members to the club of focal adhesion proteins. *Trends Cell Biol.* 2009;19(10):504-513.
5. Malinin NL, Plow EF, Byzova TV. Kindlins in FERM adhesion. *Blood.* 2010;115(20): 4011-4017.
6. Bialkowska K, Ma YQ, Bledzka K, et al. The integrin co-activator Kindlin-3 is expressed and functional in a non-hematopoietic cell, the endothelial cell. *J Biol Chem.* 2010;285(24): 18640-18649.
7. Ussar S, Moser M, Widmaier M, et al. Loss of Kindlin-1 causes skin atrophy and lethal neonatal intestinal epithelial dysfunction. *PLoS Genet.* 2008;4(12):e1000289.
8. Malinin NL, Zhang L, Choi J, et al. A point mutation in KINDLIN3 ablates activation of three integrin subfamilies in humans. *Nat Med.* 2009; 15(3):313-318.
9. Svensson L, Howarth K, McDowall A, et al. Leukocyte adhesion deficiency-III is caused by mutations in KINDLIN3 affecting integrin activation. *Nat Med.* 2009;15(3):306-312.
10. Dowling JJ, Gibbs E, Russell M, et al. Kindlin-2 is an essential component of intercalated discs and is required for vertebrate cardiac structure and function. *Circ Res.* 2008;102(4):423-431.
11. Montanez E, Ussar S, Schifferer M, et al. Kindlin-2 controls bidirectional signaling of integrins. *Genes Dev.* 2008;22(10):1325-1330.
12. Ma YQ, Qin J, Wu C, Plow EF. Kindlin-2 (Mig-2): a co-activator of beta3 integrins. *J Cell Biol.* 2008; 181(3):439-446.
13. Pluskota E, Dowling JJ, Gordon N, et al. The integrin coactivator kindlin-2 plays a critical role in angiogenesis in mice and zebrafish. *Blood.* 2011; 117(18):4978-4987.
14. Moser M, Nieswandt B, Ussar S, Pozgajova M, Fässler R. Kindlin-3 is essential for integrin activation and platelet aggregation. *Nat Med.* 2008;14(3):325-330.
15. Dowling JJ, Vreede AP, Kim S, Golden J, Feldman EL. Kindlin-2 is required for myocyte elongation and is essential for myogenesis. *BMC Cell Biol.* 2008;9:36.
16. Podrez EA, Byzova TV, Febbraio M, et al. Platelet CD36 links hyperlipidemia, oxidant stress and a prothrombotic phenotype. *Nat Med.* 2007;13(9): 1086-1095.
17. Zhuo Y, Ilangovan U, Schirf V, et al. Dynamic interactions between clathrin and locally structured elements in a disordered protein mediate clathrin lattice assembly. *J Mol Biol.* 2010;404(2):274-290.
18. Bledzka K, Liu J, Xu Z, et al. Spatial coordination of kindlin-2 with talin head domain in interaction with integrin β cytoplasmic tails. *J Biol Chem.* 2012;287(29):24585-24594.
19. Robson SC. Thromboregulation by endothelial cells: significance for occlusive vascular diseases. *Arterioscler Thromb Vasc Biol.* 2001;21(7): 1251-1252.
20. Marguerie GA, Plow EF. The fibrinogen-dependent pathway of platelet aggregation. *Ann N Y Acad Sci.* 1983;408:556-566.
21. Schäfer A, Bauersachs J. Endothelial dysfunction, impaired endogenous platelet inhibition and platelet activation in diabetes and atherosclerosis. *Curr Vasc Pharmacol.* 2008;6(1):52-60.
22. Marcus AJ, Broekman MJ, Drosopoulos JH, et al. Role of CD39 (NTPDase-1) in thromboregulation, cerebroprotection, and cardioprotection. *Semin Thromb Hemost.* 2005;31(2):234-246.
23. Colgan SP, Eltzschig HK, Eckle T, Thompson LF. Physiological roles for ecto-5′-nucleotidase (CD73). *Purinergic Signal.* 2006;2(2):351-360.
24. Wang LH, Rothberg KG, Anderson RG. Mis-assembly of clathrin lattices on endosomes reveals a regulatory switch for coated pit formation. *J Cell Biol.* 1993;123(5): 1107-1117.
25. Robinson MS, Kreis TE. Recruitment of coat proteins onto Golgi membranes in intact and permeabilized cells: effects of brefeldin A and G protein activators. *Cell.* 1992;69(1):129-138.
26. McMahon HT, Boucrot E. Molecular mechanism and physiological functions of clathrin-mediated endocytosis. *Nat Rev Mol Cell Biol.* 2011;12(8): 517-533.
27. Mousavi SA, Malerød L, Berg T, Kjeken R. Clathrin-dependent endocytosis. *Biochem J.* 2004;377(Pt 1):1-16.
28. Dwyer KM, Robson SC, Nandurkar HH, et al. Thromboregulatory manifestations in human CD39 transgenic mice and the implications for thrombotic disease and transplantation. *J Clin Invest.* 2004;113(10):1440-1446.
29. Crikis S, Lu B, Murray-Segal LM, et al. Transgenic overexpression of CD39 protects against renal ischemia-reperfusion and transplant vascular injury. *Am J Transplant.* 2010;10(12):2586-2595.
30. Furukoji E, Matsumoto M, Yamashita A, et al. Adenovirus-mediated transfer of human placental ectonucleoside triphosphate diphosphohydrolase to vascular smooth muscle cells suppresses platelet aggregation in vitro and arterial thrombus formation in vivo. *Circulation.* 2005;111(6):808-815.
31. Enjyoji K, Sévigny J, Lin Y, et al. Targeted disruption of cd39/ATP diphosphohydrolase results in disordered hemostasis and thromboregulation. *Nat Med.* 1999;5(9):1010-1017.
32. Koszalka P, Ozüyaman B, Huo Y, et al. Targeted disruption of cd73/ecto-5′-nucleotidase alters thromboregulation and augments vascular inflammatory response. *Circ Res.* 2004;95(8): 814-821.
33. Li Z, Zhang G, Liu J, et al. An important role of the SRC family kinase Lyn in stimulating platelet granule secretion. *J Biol Chem.* 2010;285(17): 12559-12570.

34. Subramaniam M, Frenette PS, Saffaripour S, Johnson RC, Hynes RO, Wagner DD. Defects in hemostasis in P-selectin-deficient mice. *Blood.* 1996;87(4):1238-1242.

35. Renné T, Pozgajová M, Grüner S, et al. Defective thrombus formation in mice lacking coagulation factor XII. *J Exp Med.* 2005;202(2):271-281.

36. Bugge TH, Xiao Q, Kombrinck KW, et al. Fatal embryonic bleeding events in mice lacking tissue factor, the cell-associated initiator of blood coagulation. *Proc Natl Acad Sci U S A.* 1996; 93(13):6258-6263.

37. Papanikolaou A, Papafotika A, Murphy C, et al. Cholesterol-dependent lipid assemblies regulate the activity of the ecto-nucleotidase CD39. *J Biol Chem.* 2005;280(28):26406-26414.

38. Makiya R, Thornell LE, Stigbrand T. Placental alkaline phosphatase, a GPI-anchored protein, is clustered in clathrin-coated vesicles. *Biochem Biophys Res Commun.* 1992;183(2):803-808.

39. Abrami L, Liu S, Cosson P, Leppla SH, van der Goot FG. Anthrax toxin triggers endocytosis of its receptor via a lipid raft-mediated clathrin-dependent process. *J Cell Biol.* 2003;160(3):321-328.

40. Sandvig K, Olsnes S, Brown JE, Petersen OW, van Deurs B. Endocytosis from coated pits of Shiga toxin: a glycolipid-binding protein from Shigella dysenteriae 1. *J Cell Biol.* 1989;108(4):1331-1343.

41. Le Roy C, Wrana JL. Clathrin- and non-clathrin-mediated endocytic regulation of cell signalling. *Nat Rev Mol Cell Biol.* 2005;6(2):112-126.

42. Liu J, Fukuda K, Xu Z, et al. Structural basis of phosphoinositide binding to kindlin-2 protein pleckstrin homology domain in regulating integrin activation. *J Biol Chem.* 2011;286(50): 43334-43342.

43. Qu H, Tu Y, Shi X, et al. Kindlin-2 regulates podocyte adhesion and fibronectin matrix deposition through interactions with phosphoinositides and integrins. *J Cell Sci.* 2011; 124(Pt 6):879-891.

44. Hodivala-Dilke KM, McHugh KP, Tsakiris DA, et al. Beta3-integrin-deficient mice are a model for Glanzmann thrombasthenia showing placental defects and reduced survival. *J Clin Invest.* 1999; 103(2):229-238.

45. Pinsky DJ, Broekman MJ, Peschon JJ, et al. Elucidation of the thromboregulatory role of CD39/ ectoapyrase in the ischemic brain. *J Clin Invest.* 2002;109(8):1031-1040.

46. Gayle RB III, Maliszewski CR, Gimpel SD, et al. Inhibition of platelet function by recombinant soluble ecto-ADPase/CD39. *J Clin Invest.* 1998; 101(9):1851-1859.